

Vacuum Gauge from Ultrathin MoS₂ Transistor



A. Di Bartolomeo, A. Pelella, A. Grillo, F. Urban, L. Iemmo, E. Faella, N. Martucciello, and F. Giubileo

Abstract We fabricate monolayer MoS₂ field effect transistors and study their electrical characteristics from 10⁻⁶ Torr to atmospheric air pressure. We show that the threshold voltage increases for growing pressure. Hence, we propose the transistors as air pressure sensors, showing that they are suitable as low-power vacuum gauges. The devices operate on the pressure-dependent O₂, N₂ and H₂O molecule adsorption that affects the n-doping of the MoS₂ channel.

Keywords Molybdenum disulfide · 2D materials · Transistors · Pressure sensor · Adsorbates

1 Introduction

Following the great success of graphene [1–4], several families of atomically thin materials have emerged in the past decades and have been dominating the material research scenario [5, 6]. In particular, two-dimensional (2D) transition metal dichalcogenides (TMDs) have attracted a lot of attention due to several promising properties for electronic, optoelectronic, energy, catalysis and sensing applications [7–9]. TMDs consist of a “sandwich” layered structure with a transition-metal sheet located in between two chalcogen sheets and possess unique properties such as energy bandgap tunable by the number of layers (from 0 to about 2.2 eV), good mobility up to few hundreds cm²V⁻¹ s⁻¹, photoluminescence, broadband light adsorption, surface without out-of-plane dangling bonds that allows the fabrication of heterostructures, high strength with Young’s modulus up to 300 GPa, exceptional flexibility, and thermal stability in air [10–12]. They can be produced by mechanical or liquid

A. Di Bartolomeo (✉) · A. Pelella · A. Grillo · F. Urban · L. Iemmo · E. Faella
Dipartimento di Fisica “E.R. Caianiello”, via Giovanni Paolo II, 132, 84084 Fisciano, Salerno, Italy
e-mail: adibartolomeo@unisa.it

A. Di Bartolomeo · A. Pelella · A. Grillo · F. Urban · L. Iemmo · E. Faella · N. Martucciello · F. Giubileo
CNR-Spin, via Giovanni Paolo II, 132, 84084 Fisciano, Salerno, Italy

© The Author(s), under exclusive license to Springer Nature Switzerland AG 2021
G. Di Francia and C. Di Natale (eds.), *Sensors and Microsystems*,
Lecture Notes in Electrical Engineering 753,
https://doi.org/10.1007/978-3-030-69551-4_7

exfoliation, chemical vapor deposition (CVD), molecular beam epitaxy, pulsed laser deposition, etc. [13].

Molybdenum disulfide (MoS_2) is formed by covalently bonded S–Mo–S sequences held together by weak van der Waals forces, resulting in easy-to-exfoliate 2D layers [14, 15]. MoS_2 is a semiconductor with 1.2 eV indirect bandgap in the bulk form that widens up to 1.8–1.9 eV and becomes direct in the monolayer. It is a promising material for field-effect transistors (FETs) with high performance and on/off ratio [16–18], sensitive broadband photodetectors [19, 20], catalysis [21], chemical and biological [22–25] or strain and pressure sensors [23, 26].

Microscopic pressure sensors that can rapidly detect small pressure variations are of high demand in robotic technologies, human–machine interfaces, electronic skin, sound wave detection, and health monitoring devices. Pressure sensors are very important in many other fields, such as automobiles, aircrafts, well drilling, and medical applications.

The exceptional mechanical properties of MoS_2 nanosheets [27] have inspired their application as ultrathin diaphragms capable of large deflection deformations at low pressure to achieve high sensitivity in pressure sensors. For instance, a thin and sensitive diaphragm is attached onto one end face of a cleaved optical fiber to form an extrinsic Fabry–Perot interferometric structure that detects the applied pressure through the measurement of the deflection deformation of the diaphragm. Fabry–Perot ultrasensitive pressure sensors with nearly synchronous pressure–deflection responses have been fabricated using few-layer MoS_2 films. Compared to conventional diaphragm materials (e.g., silica, silver films), they have allowed to achieve three orders of magnitude higher sensitivity (89.3 nm Pa^{-1}) [28].

Highly sensitive pressure sensors have been fabricated by integrating a conductive microstructured air-gap gate with MoS_2 transistors. The air-gap gate is used as the pressure-sensitive gate for 2D MoS_2 transistors to reach pressure sensitivity amplification to $\sim 10^3\text{--}10^7 \text{ kPa}^{-1}$ at an optimized pressure regime of $\sim 1.5 \text{ kPa}$ [29].

Due to the atomic thickness, the electrical properties of two-dimensional materials are highly affected by ambient gases and their pressure variations. The adsorbed gas modifies the electron states within 2D materials changing their electrical conductivity. Owing to the low adsorption energy the process can be reversible.

Specifically, it has been demonstrated that MoS_2 conductivity can be enhanced or suppressed by gases such as O_2 , CH_4 , NO_2 , NO , NH_3 , H_2S , etc. [22, 30, 31]. Therefore, few- and single-layer MoS_2 nanosheets have been investigated for gas and pressure sensing in devices with fast response speed, low power consumption, low minimum pressure detection limits and excellent stability. For instance, few-layer MoS_2 back-gate field effect transistors, fabricated on SiO_2/Si substrate with Au electrodes, have been demonstrated as resistor-based O_2 sensors with sensing performance controllable by the back-gate voltage. Remarkably, these devices have been applied to determine O_2 partial pressure with a detectability as low as 6.7×10^{-7} millibars at a constant vacuum pressure and proposed as a vacuum gauge [32].

In this paper, we fabricate MoS_2 back-gate field effect transistors using MoS_2 nanosheets grown by chemical vapor deposition (CVD) on SiO_2/Si substrate and measure their electrical characteristics at different air pressures. We show that the

threshold voltage of the transistors increases with the increasing pressure. We ascribe such a feature to pressure-dependent adsorption of electronegative oxygen, nitrogen and water molecules, which decrease the n-doping of the MoS₂ channel and hence increase the threshold voltage of the transistors. We propose to exploit the dependence of the transistor current on the air pressure to realize vacuum gauges with wide dynamic range and low power consumption.

2 Experimental

The MoS₂ monolayer flakes were grown by CVD on a heavily doped Si substrate covered by 285 nm SiO₂, spin coated with 1% sodium cholate solution. The molybdenum needed for the growth was provided by a saturated ammonium heptamolybdate (AHM) solution, which was annealed at 300 °C under ambient conditions to turn AHM into MoO₃. The substrate and the AHM solution were placed in a three-zone tube furnace, along with 50 mg of S powder, positioned upstream in a separate heating zone. The zones containing the S and the AHM were heated to 150 °C and 750 °C, respectively. After 15 min of growth, the process was stopped, and the sample cooled down rapidly.

MoS₂ nanoflakes with different shapes and thicknesses, depending on both the local stoichiometry and temperature, were formed [33]. An example is shown in Fig. 1a.

We used optical microscope inspection, with contrast calibrated to approximately estimate the number of layers, to identify MoS₂ nanoflakes suitable for the transistor fabrication. A standard e-beam lithography and lift-off process was applied to evaporate Ti (10 nm) and Au (40 nm) bilayers on the flake for the formation of the source and drain electrodes. The back-gate electrode was formed by scratching the Si substrate surface and dropping silver paste.

The SEM top view of a typical device, fabricated using a star-like nanoflake, is shown in Fig. 1a. Figure 1b shows the Raman spectrum of the flake under 532 nm laser excitation. The wavenumber difference, $\Delta k \approx 20.8 \text{ cm}^{-1}$, between the E_{2g}^1 (in-plane optical vibration of S atoms in the basal plane) and A_{1g} (out-of-plane optical vibration of S atoms along the c axis) indicates a monolayer [34, 35].

Figure 1c displays the schematic cross-section of the device and the circuits used for the electrical characterization of the transistor in common source configuration. The electrical measurements were carried out inside a cryogenic probe station with fine pressure control (Janis ST 500), connected to a Keithley 4200 SCS (source measurement units, Tektronix Inc.), at room temperature.

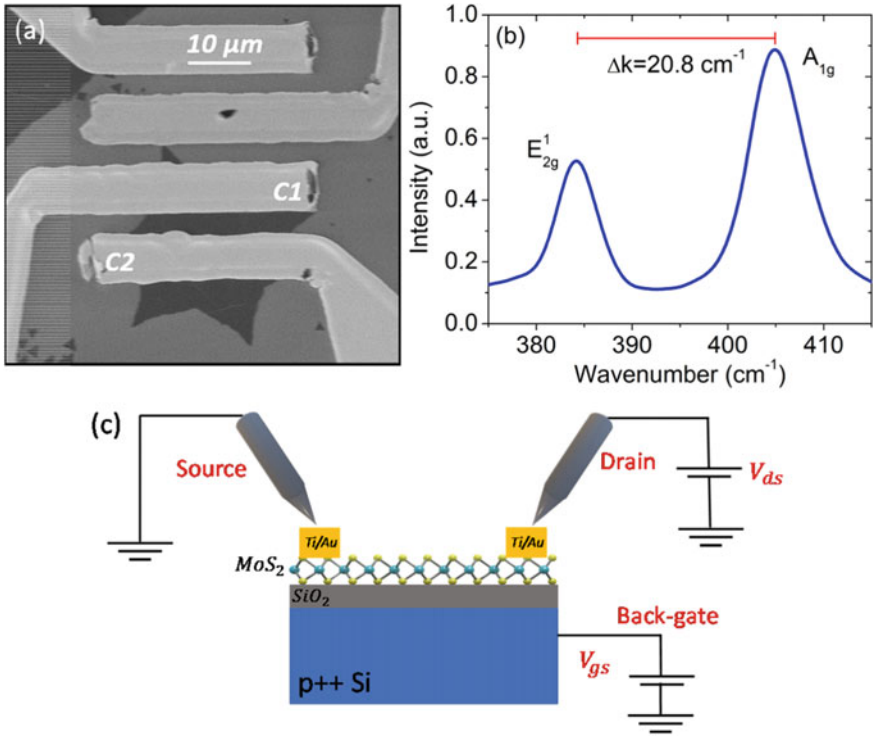


Fig. 1 **a** SEM image showing the star-like MoS₂ nanoflake used as the channel of the back-gate transistor with Ti/Au contacts. The channel width and length are 28.0 μm and 4.4 μm, respectively. **b** Raman spectrum of the MoS₂ nanoflake with $E_{2g}^1 - A_{1g}$ wavenumber separation corresponding to a monolayer. **c** MoS₂ FET schematic with biasing circuits used for the electrical characterization

3 Results and Discussion

Figure 2a, b show the $I_{ds} - V_{ds}$ output characteristics and the $I_{ds} - V_{gs}$ transfer characteristics of the MoS₂ transistor measured in high vacuum and at room temperature. As often observed in MoS₂ and other 2D-material based devices, the output characteristic exhibits an asymmetric behavior for positive and negative drain biases. As we have demonstrated elsewhere, such a feature is caused by the different contact area as well as by a difference in the Schottky barrier height at the two contacts resulting from local MoS₂ processing or intrinsic defects [36, 37]. The transfer characteristic shows a normally-on, n-type transistor. The intrinsic n-type conduction is typical of MoS₂ and is mainly due to S vacancies [38]. Compared to similar devices reported in the literature, the transistor shows good metrics in terms of on/off ratio 10^8 at ± 60 V, on-current $\sim 0.3 \frac{\mu A}{\mu m}$, subthreshold swing of $3.5 \frac{V}{\text{decade}}$ and mobility $\mu = \frac{L}{WC_{ox} V_{ds}} \frac{dI_{ds}}{dV_{gs}} \approx 1.2 \text{ cm}^2 \text{ V}^{-1} \text{ s}^{-1}$ (L and W are the channel length and width,

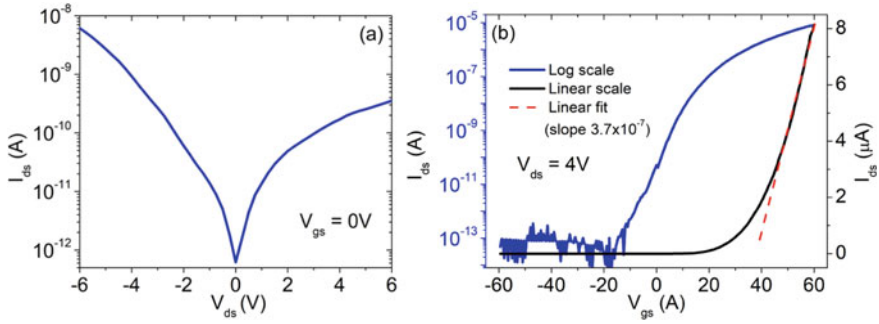


Fig. 2 **a** Output and **b** transfer (on linear and logarithmic scale) characteristics of the device between C1 and C2 contacts measured at room temperature and 10^{-6} Torr pressure. The dashed red line is a linear fit used to evaluate the channel field effect mobility

V_{ds} is the source-drain bias and $C_{ox} = 12.1 \text{ nF cm}^{-2}$ is the SiO_2 capacitance per unit area) [39–41].

The result of transfer characteristic measurements at different pressures, P , from high vacuum to atmospheric pressure and back to 10^{-6} Torr, is displayed in Fig. 3a. The increasing air pressure causes a right-shift of the transfer curve and therefore an increase of transistor threshold voltage, V_{th} . The threshold voltage is here defined as the x-axis intercept of the straight lines fitting the $I_{ds} - V_{ds}$ curves in the current range 1–100 nA. The effect is reversible, in fact the device returns to the pristine state when the high vacuum is restored, as shown by the dash-dot grey line in Fig. 3a. We note that the effect of air pressure on the channel conductance, which could result in the dramatic transformation of n-type to p-type conduction when passing from high vacuum to atmospheric pressure, has been reported also for other 2D TMDs

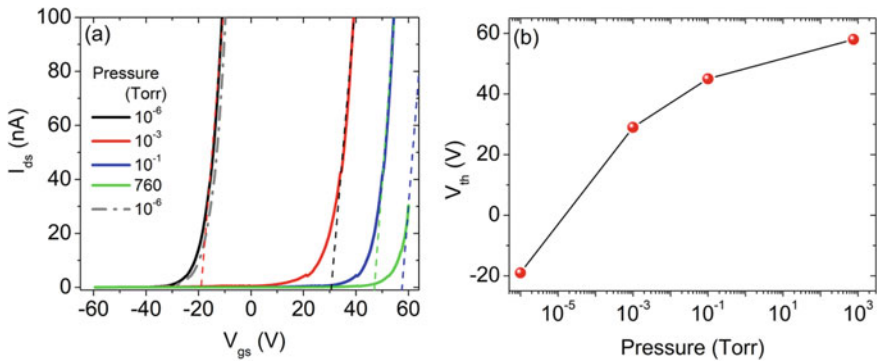


Fig. 3 **a** Transfer characteristics (solid lines) on linear scale for increasing pressure from high vacuum to atmospheric. The dashed lines are linear fits used to evaluate the transistor threshold voltage. The dash-dot gray line is obtained after that the high vacuum is restored. **b** Threshold voltage as a function of the pressure (color figure online)

materials such as WSe_2 or PdSe_2 [11, 42]. The effect is usually reversible although it has been found that an aging can occur in specific TMDs, such as PdSe_2 , after a long (>20 days) air exposure at atmospheric pressure [43].

The monotonic $V_{th} - P$ behaviour, shown in Fig. 3b, suggests that the transistor can be used as pressure sensor, with maximum sensitivity up to $\frac{dV}{d(\log_{10} P)} \approx 13 \frac{\text{V}}{\text{decade}}$ at lower pressures, where the $V_{th} - P$ curve is steeper. Besides the higher sensitivity, the duty cycle of the device increases when operated in vacuum because of the suppressed air aging effect. Therefore, the sensor is best suited as a vacuum gauge. Moreover, low current of 1 nA or less is needed to monitor the V_{th} variation, which implies that the sensor can be operated in low power-consumption regime.

To investigate the working principle of the device, we measured the transfer characteristics over a gate voltage loop (backward and forward sweep) in air and vacuum. Figure 4a shows the appearance of a hysteresis that diminishes for decreasing pressure. Hysteresis is a well-known phenomenon in transistors with 2D material channels and has been attributed to charge trapping in intrinsic defects of the 2D material, in the gate dielectric and in adsorbate molecules [38, 40, 44–46]. The reducing hysteresis with pressure confirms that adsorbates play an important role in the device under study.

Owing to their high electronegativity, molecular O_2 , N_2 and H_2O , adsorbed on MoS_2 surface (Fig. 4b), can withdraw electrons from the channel causing the observed increase of the threshold voltage, i.e. of the gate voltage needed to enable conduction in the transistor channel. Absorption occurs particularly at S vacancy sites and the absorption/desorption rate obviously depends on the air pressure the MoS_2 nanosheet is exposed to, thus enabling its monitoring.

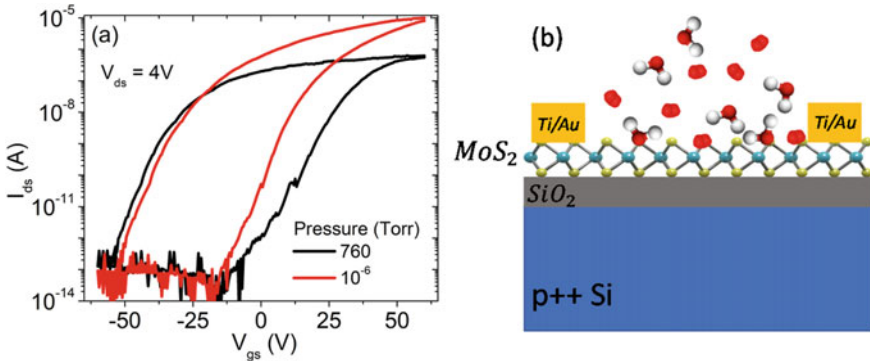


Fig. 4 **a** Transfer characteristics showing a hysteresis between the forward and reverse V_{gs} sweeps. The hysteresis width decreases for lowering pressure from atmospheric to 10^{-6} Torr. **b** Schematic showing the adsorption of molecular O_2 and H_2O which, being electronegative, cause the decrease of the electron density in the transistor channel and an increase of the threshold voltage

4 Conclusion

We have fabricated and electrically characterized monolayer MoS₂ field effect transistors. We have found that the threshold voltage of the transistors increases monotonously with the air pressure, as effect of reduced n-doping caused by adsorption of electronegative O₂, N₂ and water. Therefore, we have proposed the transistors as air pressure sensors, highlighting their suitability as a vacuum gauge with long duty cycle and low power consumption.

References

1. Geim AK, Novoselov KS (2007) The rise of graphene. *Nat Mater* 6:183–191. <https://doi.org/10.1038/nmat1849>
2. Di Bartolomeo A (2016) Graphene Schottky diodes: an experimental review of the rectifying graphene/semiconductor heterojunction. *Phys Rep* 606:1–58. <https://doi.org/10.1016/j.physrep.2015.10.003>
3. Allen MJ, Tung VC, Kaner RB (2010) Honeycomb carbon: a review of graphene. *Chem Rev* 110:132–145. <https://doi.org/10.1021/cr900070d>
4. Urban F, Lupina G, Grillo A, Martucciello N, Di Bartolomeo A (2020) Contact resistance and mobility in back-gate graphene transistors. *Nano Express* 1:010001. <https://doi.org/10.1088/2632-959X/ab7055>
5. Di Bartolomeo A (2020) Emerging 2D materials and their Van Der Waals heterostructures. *Nanomaterials* 10:579. <https://doi.org/10.3390/nano10030579>
6. Novoselov KS, Mishchenko A, Carvalho A, Castro Neto AH (2016) 2D materials and van der Waals heterostructures. *Science* 353:aac9439. <https://doi.org/10.1126/science.aac9439>
7. Choi W, Choudhary N, Han GH, Park J, Akinwande D, Lee YH (2017) Recent development of two-dimensional transition metal dichalcogenides and their applications. *Mater Today* 20:116–130. <https://doi.org/10.1016/j.mattod.2016.10.002>
8. Lv R, Robinson JA, Schaak RE, Sun D, Sun Y, Mallouk TE, Terrones M (2015) Transition metal dichalcogenides and beyond: synthesis, properties, and applications of single- and few-layer nanosheets. *Acc Chem Res* 48:56–64. <https://doi.org/10.1021/ar5002846>
9. Di Bartolomeo A, Urban F, Passacantando M, McEvoy N, Peters L, Iemmo L, Luongo G, Romeo F, Giubileo F (2019) A WSe₂ vertical field emission transistor. *Nanoscale* 11:1538–1548. <https://doi.org/10.1039/C8NR09068H>
10. Ravindra NM, Tang W, Rassay S (2019) Transition metal dichalcogenides properties and applications. In: Pech-Canul MI, Ravindra NM (eds) *Semiconductors*. Springer International Publishing, Cham, pp 333–396
11. Urban F, Martucciello N, Peters L, McEvoy N, Di Bartolomeo A (2018) Environmental effects on the electrical characteristics of back-gated WSe₂ field-effect transistors. *Nanomaterials* 8:901. <https://doi.org/10.3390/nano8110901>
12. Liu K, Yan Q, Chen M, Fan W, Sun Y, Suh J, Fu D, Lee S, Zhou J, Tongay S, Ji J, Neaton JB, Wu J (2014) Elastic properties of chemical-vapor-deposited monolayer MoS₂, WS₂, and their bilayer heterostructures. *Nano Lett* 14:5097–5103. <https://doi.org/10.1021/nl501793a>
13. Cai Y, Xu K, Zhu W (2018) Synthesis of transition metal dichalcogenides and their heterostructures. *Mater Res Express* 5:095904. <https://doi.org/10.1088/2053-1591/aad950>
14. Krishnan U, Kaur M, Singh K, Kumar M, Kumar A (2019) A synoptic review of MoS₂: synthesis to applications. *Superlattices Microstruct* 128:274–297. <https://doi.org/10.1016/j.spmi.2019.02.005>

15. Li X, Zhu H (2015) Two-dimensional MoS₂: properties, preparation, and applications. *J Materiomics* 1:33–44. <https://doi.org/10.1016/j.jmat.2015.03.003>
16. Iemmo L, Urban F, Giubileo F, Passacantando M, Di Bartolomeo A (2020) Nanotip contacts for electric transport and field emission characterization of ultrathin MoS₂ flakes. *Nanomaterials* 10:106. <https://doi.org/10.3390/nano10010106>
17. Kwon H, Garg S, Park JH, Jeong Y, Yu S, Kim SM, Kung P, Im S (2019) Monolayer MoS₂ field-effect transistors patterned by photolithography for active matrix pixels in organic light-emitting diodes. *npj 2D Mater Appl* 3:9. <https://doi.org/10.1038/s41699-019-0091-9>
18. Giubileo F, Iemmo L, Passacantando M, Urban F, Luongo G, Sun L, Amato G, Enrico E, Di Bartolomeo A (2019) Effect of electron irradiation on the transport and field emission properties of few-layer MoS₂ field-effect transistors. *J Phys Chem C* 123:1454–1461. <https://doi.org/10.1021/acs.jpcc.8b09089>
19. Gant P, Huang P, Pérez de Lara D, Guo D, Frisenda R, Castellanos-Gomez A (2019) A strain tunable single-layer MoS₂ photodetector. *Mater Today* 27:8–13. <https://doi.org/10.1016/j.mat.tod.2019.04.019>
20. Di Bartolomeo A, Genovese L, Foller T, Giubileo F, Luongo G, Croin L, Liang S-J, Ang LK, Schleberger M (2017) Electrical transport and persistent photoconductivity in monolayer MoS₂ phototransistors. *Nanotechnology* 28:214002. <https://doi.org/10.1088/1361-6528/aa6d98>
21. Madauß L, Zegkinoglou I, Vázquez Muiños H, Choi Y-W, Kunze S, Zhao M-Q, Naylor CH, Ernst P, Pollmann E, Ochedowski O, Lebius H, Benyagoub A, Ban-d'Etat B, Johnson ATC, Djurabekova F, Roldan Cuenya B, Schleberger M (2018) Highly active single-layer MoS₂ catalysts synthesized by swift heavy ion irradiation. *Nanoscale* 10:22908–22916. <https://doi.org/10.1039/C8NR04696D>
22. Li W, Zhang Y, Long X, Cao J, Xin X, Guan X, Peng J, Zheng X (2019) Gas sensors based on mechanically exfoliated MoS₂ nanosheets for room-temperature NO₂ detection. *Sensors* 19:2123. <https://doi.org/10.3390/s19092123>
23. Park M, Park YJ, Chen X, Park Y-K, Kim M-S, Ahn J-H (2016) MoS₂-based tactile sensor for electronic skin applications. *Adv Mater* 28:2556–2562. <https://doi.org/10.1002/adma.201505124>
24. Zhang W, Zhang P, Su Z, Wei G (2015) Synthesis and sensor applications of MoS₂-based nanocomposites. *Nanoscale* 7:18364–18378. <https://doi.org/10.1039/C5NR06121K>
25. Kalantar-zadeh K, Ou JZ (2016) Biosensors based on two-dimensional MoS₂. *ACS Sens* 1:5–16. <https://doi.org/10.1021/acssensors.5b00142>
26. Kim SJ, Mondal S, Min BK, Choi C-G (2018) Highly sensitive and flexible strain-pressure sensors with cracked paddy-shaped MoS₂/graphene foam/ecoflex hybrid nanostructures. *ACS Appl Mater Interfaces* 10:36377–36384. <https://doi.org/10.1021/acsami.8b11233>
27. Akhter MJ, Kuś W, Mrozek A, Burczyński T (2020) Mechanical properties of monolayer MoS₂ with randomly distributed defects. *Materials* 13:1307. <https://doi.org/10.3390/ma13061307>
28. Yu F, Liu Q, Gan X, Hu M, Zhang T, Li C, Kang F, Terrones M, Lv R (2017) Ultrasensitive pressure detection of few-layer MoS₂. *Adv Mater* 29:1603266. <https://doi.org/10.1002/adma.201603266>
29. Huang Y-C, Liu Y, Ma C, Cheng H-C, He Q, Wu H, Wang C, Lin C-Y, Huang Y, Duan X (2020) Sensitive pressure sensors based on conductive microstructured air-gap gates and two-dimensional semiconductor transistors. *Nat Electron* 3:59–69. <https://doi.org/10.1038/s41928-019-0356-5>
30. Park J, Mun J, Shin J-S, Kang S-W (2018) Highly sensitive two-dimensional MoS₂ gas sensor decorated with Pt nanoparticles. *R Soc Open Sci* 5:181462. <https://doi.org/10.1098/rsos.181462>
31. Urban F, Giubileo F, Grillo A, Iemmo L, Luongo G, Passacantando M, Foller T, Madauß L, Pollmann E, Geller MP, Oing D, Schleberger M, Di Bartolomeo A (2019) Gas dependent hysteresis in MoS₂ field effect transistors. *2D Mater* 6:045049. <https://doi.org/10.1088/2053-1583/ab4020>
32. Tong Y, Lin Z, Thong JTL, Chan DSH, Zhu C (2015) MoS₂ oxygen sensor with gate voltage stress induced performance enhancement. *Appl Phys Lett* 107:123105. <https://doi.org/10.1063/1.4931494>

33. Wang L, Chen F, Ji X (2017) Shape consistency of MoS₂ flakes grown using chemical vapor deposition. *Appl Phys Express* 10:065201. <https://doi.org/10.7567/APEX.10.065201>
34. Gołasa K, Grzeszczuk M, Korona KP, Bożek R, Binder J, Szczytko J, Wyszomerek A, Babiński A (2013) Optical properties of molybdenum disulfide (MoS₂). *Acta Phys Pol A* 124:849–851. <https://doi.org/10.12693/APhysPolA.124.849>
35. Zeng H, Zhu B, Liu K, Fan J, Cui X, Zhang QM (2012) Low-frequency Raman modes and electronic excitations in atomically thin MoS₂ films. *Phys Rev B* 86:241301. <https://doi.org/10.1103/PhysRevB.86.241301>
36. Di Bartolomeo A, Grillo A, Urban F, Iemmo L, Giubileo F, Luongo G, Amato G, Croin L, Sun L, Liang S-J, Ang LK (2018) Asymmetric Schottky contacts in bilayer MoS₂ field effect transistors. *Adv Funct Mater* 28:1800657. <https://doi.org/10.1002/adfm.201800657>
37. Di Bartolomeo A, Giubileo F, Grillo A, Luongo G, Iemmo L, Urban F, Lozzi L, Capista D, Nardone M, Passacantando M (2019) Bias tunable photocurrent in metal-insulator-semiconductor heterostructures with photoresponse enhanced by carbon nanotubes. *Nanomaterials* 9:1598. <https://doi.org/10.3390/nano9111598>
38. Di Bartolomeo A, Genovese L, Giubileo F, Iemmo L, Luongo G, Foller T, Schleberger M (2017) Hysteresis in the transfer characteristics of MoS₂ transistors. *2D Mater* 5:015014. <https://doi.org/10.1088/2053-1583/aa91a7>
39. Yuan H, Cheng G, You L, Li H, Zhu H, Li W, Kopanski JJ, Obeng YS, Hight Walker AR, Gundlach DJ, Richter CA, Ioannou DE, Li Q (2015) Influence of metal–MoS₂ interface on MoS₂ transistor performance: comparison of Ag and Ti contacts. *ACS Appl Mater Interfaces* 7:1180–1187. <https://doi.org/10.1021/am506921y>
40. Ahn J-H, Parkin WM, Naylor CH, Johnson ATC, Drndić M (2017) Ambient effects on electrical characteristics of CVD-grown monolayer MoS₂ field-effect transistors. *Sci Rep* 7:4075. <https://doi.org/10.1038/s41598-017-04350-z>
41. Grillo A, Di Bartolomeo A, Urban F, Passacantando M, Caridad JM, Sun J, Camilli L (2020) Observation of 2D conduction in ultrathin germanium arsenide field-effect transistors. *ACS Appl Mater Interfaces* 12:12998–13004. <https://doi.org/10.1021/acsami.0c00348>
42. Giubileo F, Grillo A, Iemmo L, Luongo G, Urban F, Passacantando M, Di Bartolomeo A (2020) Environmental effects on transport properties of PdSe₂ field effect transistors. *Mater Today Proc* 20:50–53. <https://doi.org/10.1016/j.matpr.2019.08.226>
43. Hoffman AN, Gu Y, Liang L, Fowlkes JD, Xiao K, Rack PD (2019) Exploring the air stability of PdSe₂ via electrical transport measurements and defect calculations. *npj 2D Mater Appl* 3:50. <https://doi.org/10.1038/s41699-019-0132-4>
44. Di Bartolomeo A, Pelella A, Liu X, Miao F, Passacantando M, Giubileo F, Grillo A, Iemmo L, Urban F, Liang S (2019) Pressure-tunable ambipolar conduction and hysteresis in thin palladium diselenide field effect transistors. *Adv Funct Mater* 29:1902483. <https://doi.org/10.1002/adfm.201902483>
45. Kaushik N, Mackenzie DMA, Thakar K, Goyal N, Mukherjee B, Boggild P, Petersen DH, Lodha S (2017) Reversible hysteresis inversion in MoS₂ field effect transistors. *npj 2D Mater Appl* 1:34. <https://doi.org/10.1038/s41699-017-0038-y>
46. Bartolomeo AD, Rinzan M, Boyd AK, Yang Y, Guadagno L, Giubileo F, Barbara P (2010) Electrical properties and memory effects of field-effect transistors from networks of single- and double-walled carbon nanotubes. *Nanotechnology* 21:115204. <https://doi.org/10.1088/0957-4484/21/11/115204>